

## The role of co-simulation in the integrated design of high-dynamics servomechanisms: an experimental evaluation

M. Pellicciari<sup>1, a</sup>, G. Berselli<sup>1, b</sup>, M. Ori<sup>1, c</sup>, F. Leali<sup>1, d</sup>

<sup>1</sup>DIEF Department of Engineering "Enzo Ferrari" - University of Modena and Reggio Emilia  
Via Vignolese 905, 41125 Modena, ITALY

<sup>a</sup>marcello.pellicciari@unimore.it, <sup>b</sup>giovanni.berselli@unimore.it, <sup>c</sup>mirko.ori@unimore.it,  
<sup>d</sup>francesco.leali@unimore.it

**Keywords:** Virtual prototyping, integrated mechatronic design, co-simulation, digital product design.

**Abstract.** This paper reports about the design and modeling process of high performance servo-actuated mechanisms for automatic machines. Besides being a delicate and time consuming process, coupled simulations based on virtual prototyping finally offer the chance to integrate engineering methods proper of control system engineering and mechanical design. In particular, the main target of this work is to investigate how different virtual prototyping approaches, each having increasing level of detail, can contribute to the appropriate prediction of the expected machine performance. These results are then compared with experimental data obtained on a real servomechanism prototype. The comparison quantitatively demonstrates the improvement on torque prediction and position error reduction when detailed models of the controller and the electric motor dynamics are coupled with the mechanical system model.

### Introduction

Modern manufacturing systems, as well as automatic machines for packaging, are required to achieve high dynamics and precise motions, traditionally accomplished by means of custom designed fully-mechanical drives (e.g. mechanical cams). This traditional approach leads to machine architectures specifically optimized for single motion laws, hence limiting the achieved performance to single tasks. On the other hand, future manufacturing systems will require high flexibility and reconfigurability in order to adapt to ever changing production scenarios [1-3]. Therefore, last generation designs aim at substituting fully-mechanical drives with multipurpose and programmable Servo-actuated Mechanisms (SM).

The adoption of these programmable SM introduces new engineering challenges, mainly related to the limited stiffness and motion dynamics, that usually require intensive experimental tuning [4]. In this context, in order to gain performance comparable to mechanical drives by means of modern mechatronic systems, the synergistic contributions of both mechanism structure and servo actuation must be exploited. Nonetheless, at the state-of-the-art, SM are de facto designed and developed with concurrent tools and methods, which are intrinsically separated and hardly integrated.

In theory, a better design process would rely on coupled simulation based on virtual prototyping, which now offers the chance to integrate control engineering and mechanical design methods. In any case, co-simulation is still a delicate, complex and time consuming process as long as high detailed virtual prototypes require difficult tuning of the model parameters and may lead to undesired errors. Basically, for an effective and concretely exploitable design practice, such virtual prototypes should only integrate the behavioral models strictly needed to support design and optimization of the overall system. Henceforth, it becomes fundamental to investigate the real effectiveness of different simulations approaches, each having different level of detail, and to compare their contribution to the appropriate prediction of the expected performance.

**Servo actuated mechanisms design.** Regardless the machine architecture, a complex automatic machine may be divided into simpler subsystems which, in most cases, operate with one degree of freedom (d.o.f.) only. With reference to Fig. 1, a single d.o.f. SM can be defined as a mechatronic system whose overall performances are determined by the synergistic integration of: a) mechanical

system kinematics/dynamics (load); b) electric drive, comprising a power converter, a controller, an electric gear-motor and suitable sensors; c) motion laws programmed within the controller. As for the electric motor, Permanent Magnet synchronous Motors (PMM) are today the de facto industry standard for position controlled servo systems [5]. Note that, owing to the high-precision requirements, only direct-drive solutions will be considered in the following.

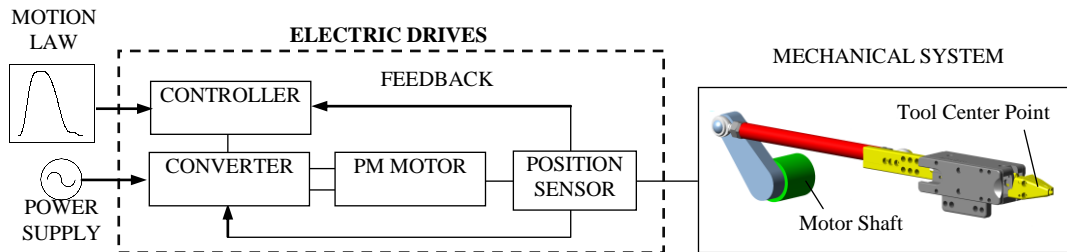


Fig. 1 – Schematic of a single d.o.f. servomechanism.

As said, SM (and automatic machines in general) are firstly designed by mechanical engineers with the aid of CAD software. The mechanical system is then optimized by means of Multi-Body Dynamics (MBD) simulations and Finite Element Methods (FEM). In parallel, the motion laws and the tuning of the control parameters [6] are developed by control engineers focusing on the manufacturing process. Usually, the choice of the actuator model and size is separately carried out by control engineers, who import the desired motion laws and optimize the servo control. Unfortunately, every parameter and design choice adopted by the concurrent development teams has strong influence on the final system performance. Henceforth, an integrated design environment is strongly needed which is capable to predict the influence of design choices belonging to different engineering domains.

### Servo-actuated mechanism modeling

**Modeling of the rigid-body mechanism dynamics.** Given  $\vartheta(t), \dot{\vartheta}(t), \ddot{\vartheta}(t)$  which are, respectively, position, velocity and acceleration of the motor shaft as a function of time,  $t$ , the equation of motion of a generic 1 d.o.f. mechanism can be effectively described by the following relation [7]:

$$M_m = M_r + J_r(\vartheta)\ddot{\vartheta} + \frac{1}{2} \frac{dJ_r(\vartheta)}{d\vartheta} \dot{\vartheta}^2 + \frac{dW}{d\vartheta} \quad (1)$$

where  $M_m$  is the motor torque,  $M_r$  is a non-potential generalized force referred to the motor shaft (whose work equals the work of the overall system of non-potential forces and moments acting on the mechanism),  $J_r$  is the reduced moment of inertia, and  $W$  is the potential energy stored in the mechanism. It is worth noting that  $J_r(\vartheta)$  is always positive and its value is independent of the direction of motion. Once the parameters concerning the inertial properties of the moving links are known, the quantities on the right-hand-side of Eq. 1 can be computed by means of either general-purpose MBD software [8], whose usage can effectively speed-up time consuming calculation even in case of very simple closed-loop mechanisms [9], or following well known procedures outlined, for instance, in [7].

**Modeling the SM control architecture.** With reference to Fig. 2, the controller of electrical drive system with PMM is usually based on a cascade structure with a fast inner loop for current control, and outer closed-loops for speed and position control. This scheme improves the robustness of the controller with respect to unavoidable modeling errors and disturbances. In the following, with obvious notation of symbols, generic actual values are referred to as  $x$  whereas reference (desired) values are written as  $x^*$ .

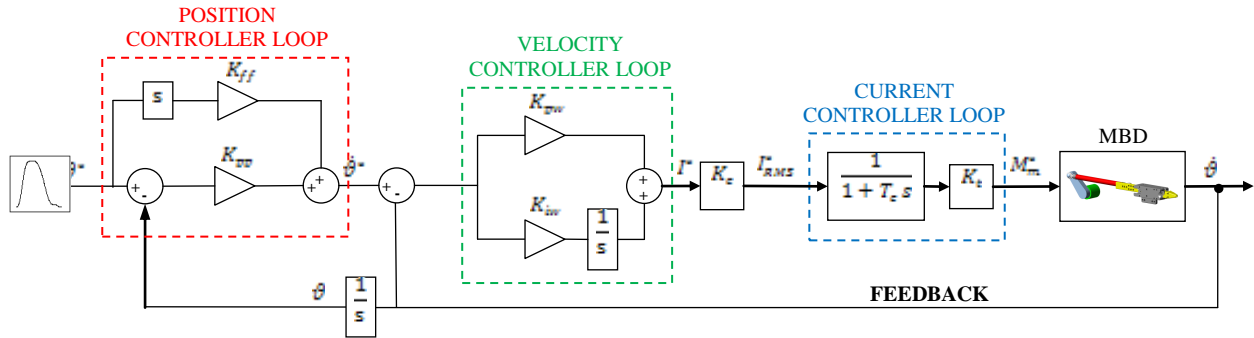


Fig. 2 – Schematic of a SM control architecture.

Concerning the speed controller, it is usually designed as a simple Proportional-Integral (PI) controller,  $K_{pw}$  and  $K_{iw}$  being the proportional and integral gains respectively. Concerning the position loop, a Proportional (P) controller with velocity feed-forward is implemented,  $K_{pp}$  and  $K_{ff}$  being the proportional and feed-forward gains respectively. As for the current loop, field oriented control in  $d-q$  frame [5] is generally implemented. In first approximation, and similarly to [4], the current loop can be model on  $q$ -axis by a first order transfer function, such that:

$$M_m^* = I_{RMS}^* K_t / (1 + T_c s) = I^* K_c K_t / (1 + T_c s) \quad (2)$$

where  $M_m^*$  is the desired motor torque,  $I_{RMS}^*$  is the RMS current in the motor,  $K_t$  is the motor torque constant (usually given by manufacturer), that is the torque produce for a given RMS current,  $K_c$  simply converts the current controller output,  $I^*$ , into motor current in Ampere, and  $T_c$  is the time constant which approximates the current loop dynamics. Note that, in Eq. 2, the motor dynamics has been neglected, the motor input current being simply proportional to the supplied torque via the torque constant  $K_t$ .

**Modeling of the PMM dynamics.** In order to improve model accuracy, the dynamics of the PMM can be included. In particular, the permanent magnets on the rotor are shaped in such a way so as to produce sinusoidal back EMF in the stator windings. Aim of the current control is to maintain the desired value of current, by managing the effect of back EMF. Similarly to [5], Fig. 3 depicts a simplified schematic of a 3-phase PMM together with a stator reference axis for the  $a$ -phase ( $b$ - and  $c$ - frames being chosen  $120^\circ$  and  $240^\circ$  ahead of the  $a$ -axis, respectively). In addition, the same figure depicts the rotor reference frame, that is the  $d-q$  frame. The  $q$ -axis is chosen  $90^\circ$  ahead of the  $d$ -axis, and the angle of the rotor  $q$ -axis with respect to the stator  $a$ -axis coincides with the motor shaft displacement  $\vartheta(t)$ . Resorting to the well-known  $dq0$  transformation [5], the following relations hold:

$$V_d = R_s I_d + L_d \frac{dI_d}{dt} - \dot{\vartheta} p L_q I_q \quad (3); \quad V_q = R_s I_q + L_q \frac{dI_q}{dt} - \dot{\vartheta} p L_d I_d + \dot{\vartheta} p \lambda_m \quad (4)$$

where  $d$  and  $q$  subscripts represent direct and quadrature stator axis respectively, whereas  $V$  is voltages,  $R_s$  is stator resistance,  $I$  is current,  $\dot{\vartheta}$  is rotor speed,  $L$  is inductance,  $p$  is number of pole pairs,  $\lambda_m = \sqrt{2} K_t / (3p)$  is peak flux linkage due to the permanent magnet. The equivalent circuits for direct and quadrature axis are reported in Fig. 4. The produced torque, calculated as power divided by output shaft velocity, is then given by:

$$M_m^* = 3 p [\lambda_m I_q + (L_d - L_q) I_d I_q] / 2 \quad (5)$$

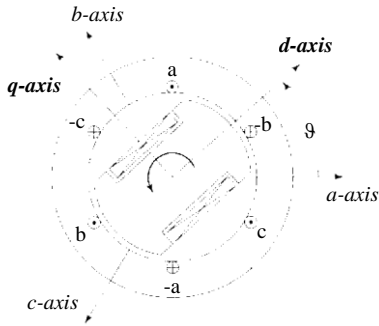


Fig. 3 – PMM schematic.

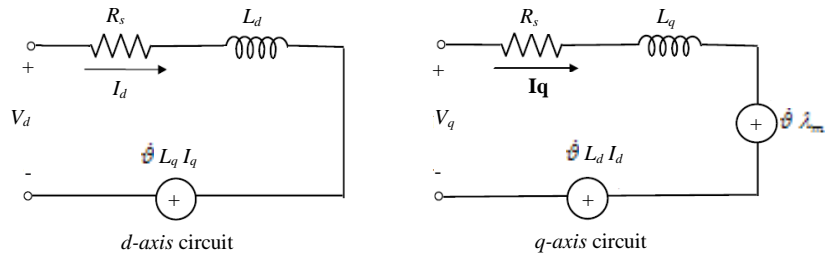


Fig. 4 – Equivalent circuits for direct and quadrature axis.

The model block diagram including PI current control in the  $d$ - $q$  frame is reported in Fig. 5 and can be employed in place of the simplified first-order current loop depicted in Fig. 2, in order to capture the influence of the PMM dynamics.

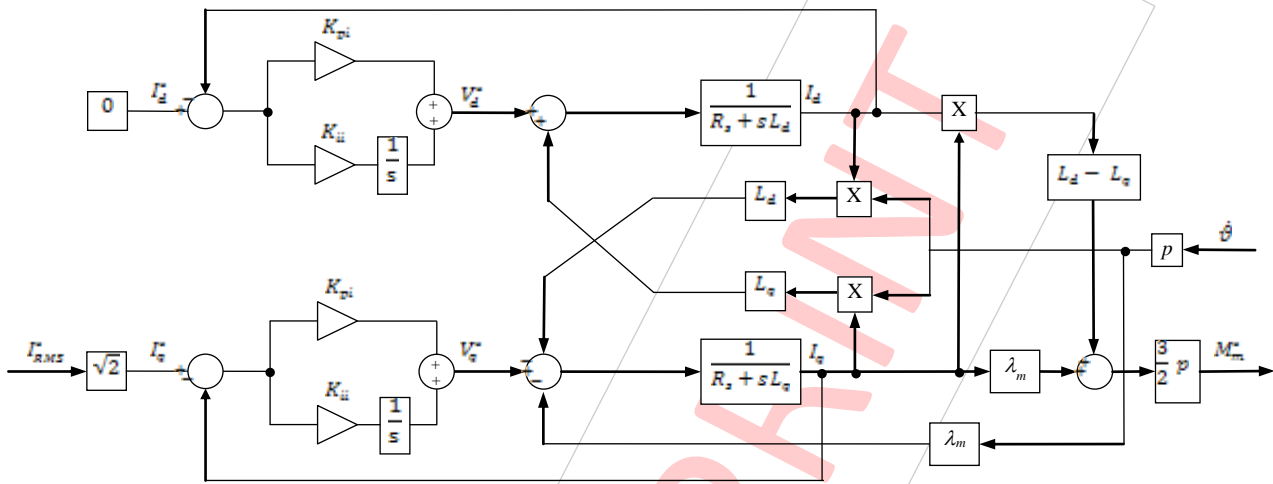


Fig. 5 – PMM dynamic model including current loop with field oriented control in  $d$ - $q$  frame [4].

**Computing the motor torque for a given task.** As shown in the previous paragraphs, the motor torque for a given motion law can be computed following three approaches with increasing level of accuracy:

- *Simulation A:* the torque required to overcome inertial and external forces on the rigid-link mechanism is computed using Eq. 1. In practice, it is supposed that reference,  $M_m^*$ , and actual torque,  $M_m$ , will be equal at any instant in time. Only the inertial properties of the mechanical system are needed in order to perform the simulation, and general-purpose MBD software can be employed [8].
- *Co-Simulation B:* the controller effect (Fig. 2) is included in co-simulation with the mechanical system. In this case, the values of the controller parameters are needed. Note that, even if in Fig. 4 the block diagrams are represented with their continuous transfer function, the actual simulation has been run implementing the sampled digital control of the real controller and position sensor ( $P_{s\text{amp}}$ ,  $V_{s\text{amp}}$ ,  $C_{s\text{amp}}$  being the sample times of position, velocity and current loop respectively).
- *Co-Simulation C:* the PMM dynamics is included and the model of Fig. 5 substitutes the control loop in Fig. 2. In this case, the motor electrical parameters must be known by either motor supplier or system identification [5].

In the following paragraph, a concrete case study will quantitatively evaluate how these three models capture the behaviour of an industrial SM in real operative conditions.

**Case study: servo-actuated slider-crank mechanism**

A slider-crank servo-actuated mechanism (Fig. 6) is taken as a reference case study for evaluating the different modeling approaches listed in the previous section. The mechanism reduced moment of inertia and its derivative along with the programmed motion law are reported in Fig. 7a and 7b. The system prototype is shown in Fig. 8. Plots are normalized with respect to their maximum values,  $t_h$  being the cycle time. Experimental results are derived at different crank speed namely 200, 300, 400, 500 RPM, the cycle time varying accordingly. As for the motor and controller parameters, data used for the co-simulation are reported in Tab. I. Also, a viscous friction with coefficient 0.06 Ns/mm has been imposed between slider and mechanism frame.

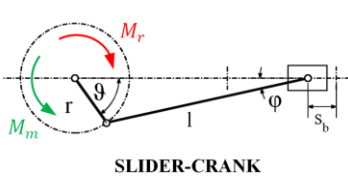


Fig. 6 – Mech. schematic.

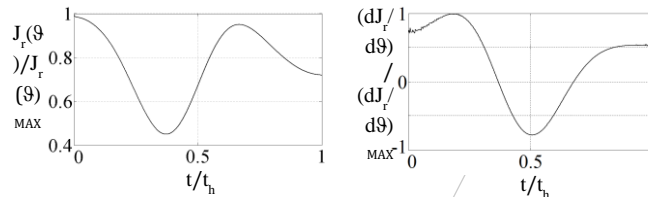


Fig. 7a – Values of  $J_r(\theta)$  and  $dJ_r/d\theta$ .



Fig. 8 – Prototype.

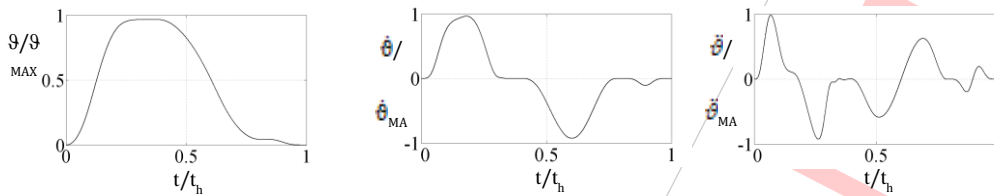


Fig. 7b – Programmed motion law (position, velocity and acceleration profiles).

Table I – Model parameters.

$p$	$R_s$ [Ω]	$L$ [mH]	$K_t$ [Nm/A]	$C_{max}$ [Nm]	$J_m$ [kgcm <sup>2</sup> ]	$K_{pp}$	$K_{ff}$	$K_{pw}$	$K_{iw}$	$K_{pc}$	$K_{ic}$	$K_c$	$T_c$ [μs]	$P_{samp}$ [μs]	$V_{samp}$ [μs]	$F_{samp}$ [μs]
4	2.6	57	5.1	114	31	25	0.98	0.09	40	160	1600	13.72	175	500	250	125

Figure 9 reports the comparison between simulated and experimental torques for  $\dot{\theta}$  equaling 200 and 500 RPM. All values are normalized by maximum experimental torque,  $M_{m,MAX}$ . In particular, Fig. 9a and 9b highlight that *Simulation A* is capable of predicting the motor torque only at low speed and can be profitably used only for first-attempt sizing the electric motor. In any case, note that the torque peak at 500 RPM is not captured, such that this modelling procedure would possibly lead to wrong actuator selection in terms of maximum torque.

The results reported in Fig. 9c and 9d are related to *Co-Simulation B* and confirm that the controller integration is essential in order to accurately predict the prototype behavior at high speed. Once again, the torque peak at 500 RPM is not fully captured. Naturally, the best results are provided by *Co-Simulation C* which, however, requires the knowledge of motor parameters which are difficult to trace on common industrial catalogues.

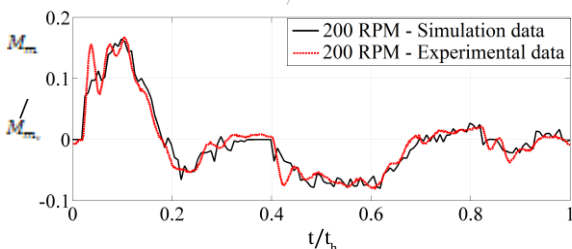


Fig. 9a – Simulation A @ 200 RPM

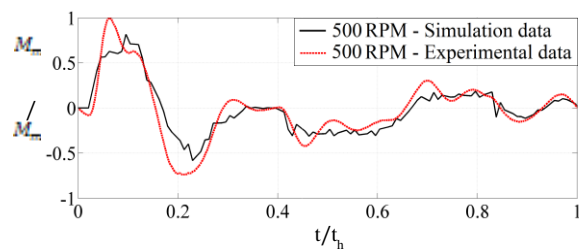


Fig. 9b – Simulation A @ 500 RPM

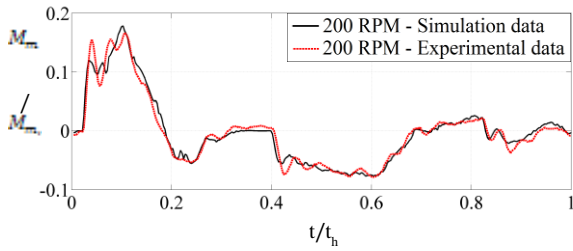


Fig. 9c – Co-Simulation B @ 200 RPM

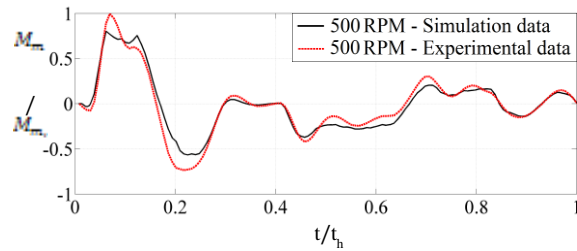


Fig. 9d – Co-Simulation B @ 500 RPM

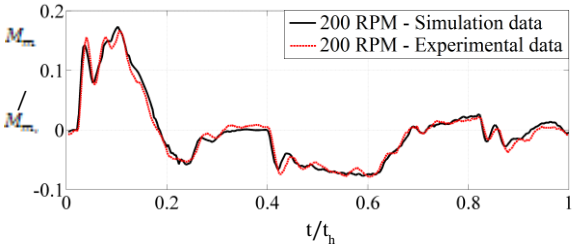


Fig. 9e – Co-Simulation C @ 200 RPM

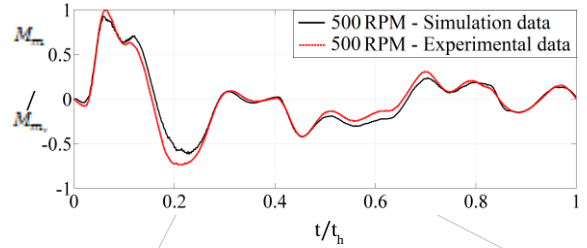


Fig. 9f – Co-Simulation C @ 500 RPM

Fig. 9 – Comparison of simulated and experimental results (@ 200 and 500 RPM) for different simulation approaches (*Simulation A*, *Co-Simulation B*, *Co-Simulation C*).

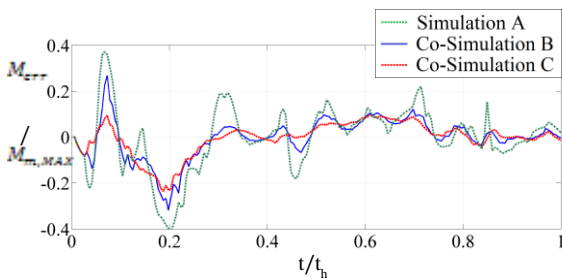


Fig. 10 – Torque error for different modeling approaches.

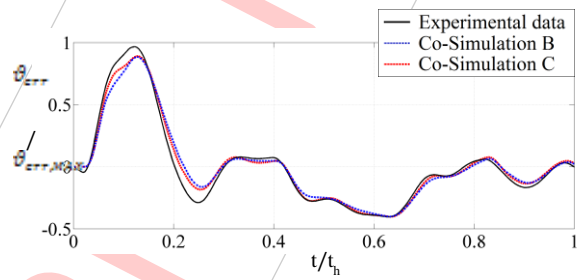


Fig. 11 – Position error for different modeling approaches.

Table II – RMS torque / position errors for different simulation approaches and varying crank speed

	RMS TORQUE ERROR [Nm]				RMS POSITION ERROR [°]			
	200 RPM	300 RPM	400 RPM	500 RPM	200 RPM	300 RPM	400 RPM	500 RPM
<i>Simulation A</i>	1.048	2.583	5.495	10.670	-	-	-	-
<i>Co-Simulation B</i>	0.765	1.531	2.786	5.984	0.137	0.242	0.282	0.343
<i>Co-Simulation C</i>	0.666	1.237	2.615	5.213	0.107	0.176	0.188	0.218

In addition, Fig. 10 reports the error between experimental and simulated data concerning *Simulation A*, and *Co-Simulation B* and *C* whereas Fig. 11 reports the position error normalized by maximum experimental error  $\theta_{err,MAX}$ , the results concerning *Simulation A* being omitted for clarity. Finally, the results for each model and for each test condition are summarize in Tab. II.

### Conclusions

This article discusses about the integrated design process of high-dynamics servo-actuated mechanism for automatic machine. In particular, three modeling approaches with increasing level of complexity and prediction accuracy are treated. Simulation results are then compared with experimental results achieved on an industrial prototype. The first approach simply models the

rigid-body dynamics of a single d.o.f. mechanism. The model prediction in terms of motor torque and Tool Center Point position show unacceptable errors at increasing speed of the mover, such that the obtained numerical results are useful only for first attempt sizing the actuation systems. Secondly, a co-simulation model including the controller architecture is discussed. Comparison with experimental results show acceptable level of accuracy even at high dynamics. At last, the electrical motor dynamics is included in the model. In this case, the number of model parameters substantially increases in parallel with an increased accuracy of the model prediction capabilities. In conclusion, the paper qualitatively show that co-simulation is a necessary step in the design of servomechanisms. The level of accuracy of the actuation system's lumped parameter model highly depends on the available data, whose determination can be extremely time consuming. Concerning future work, the dynamics of the power converter will also be included in order to potentially improve the torque prediction capabilities on one side, and to closely simulate the energy requirement of the system, on the other. In particular, with regards to the energy consumption, the authors are currently developing detailed co-simulation models of multi-d.o.f. systems such as serial [10,11] and parallel [12] robots.

## References

- [1] U. Heisel and M. Meitzner, "Progress in Reconfigurable Manufacturing Systems", J. for Manufacturing Science and Production, Vol. 6 (2011), No. 1-2, p. 1-8.
- [2] M. Pellicciari, A. O. Andrisano, F. Leali, A. Vergnano, "Engineering method for adaptive manufacturing systems design", International Journal on Interactive Design and Manufacturing, Vol. 3 (2009), No. 2, p. 81-91.
- [3] A. O. Andrisano, F. Leali, M. Pellicciari, F. Pini, A. Vergnano, "Hybrid Reconfigurable System design and optimization through virtual prototyping and digital manufacturing tools", International Journal on Interactive Design and Manufacturing, Vol. 6 (2012), No. 1, p. 17-27.
- [4] P. Pognet, M. Gautier, W. Khalil, "Modeling, Control and Simulation of High Speed Machine Tool Axes", IEEE/ASME Int. Conf. On Advanced Intelligent Mechatronics, (1999), p. 617-622.
- [5] D. Y. Ohm, "Dynamic Model of PM Synchronous Motors.", Drivetech, Inc., Blacksburg, VA. Available online: [www.drivetechinc.com](http://www.drivetechinc.com)
- [6] G. Palli, R. Carloni and C. Melchiorri, "Innovative Tools for Real-Time Simulation of Dynamic Systems", IFAC'08, 17th IFAC World Congress, Seoul, Korea, (2008).
- [7] H. Dresig and F. Holzweißig: *Dynamics of Machinery, Theory and Applications* (Springer, London 2010).
- [8] Y. Wang, Y. Gai, P. Xie, "Dynamics co-simulation of a type of spot welding robot by recurdyn and simulink", Int. Conf. on Consumer Electronics, Communications and Networks (CECNet) (2011), p. 4934-4937.
- [9] J. Ha, R. Fung, K. Chen and S. Hsien, "Dynamic modeling and identification of a slider-crank mechanism", J. of Sound and Vibration, Vol. 289 (2006), p. 1019-1044.
- [10] M. Pellicciari, G. Berselli, F. Leali, A. Vergnano, B. Lennartson, "Object-oriented Modeling of Industrial Manipulators with Application to Energy Optimal Trajectory Scaling", Proceedings of the ASME Design Engineering Technical Conference, Vol. 5 (2011), No. PARTS A AND B, p. 997-1006.
- [11] D. Meike, M. Pellicciari, G. Berselli, A. Vergnano, and L. Ribickis, "Increasing the energy efficiency of multi-robot production lines in the automotive industry", 2012 IEEE International Conference on Automation Science and Engineering, CASE 2012, Seoul, (2012), p. 696-701.
- [12] M. Pellicciari, G. Berselli, F. Leali, A. Vergnano, "A minimal touch approach for optimizing energy efficiency in pick-and-place manipulators", IEEE 15th International Conference on Advanced Robotics: New Boundaries for Robotics, ICAR 2011, Tallinn, (2011), p. 100-105.

**Advances in Mechatronics and Control Engineering**

10.4028/www.scientific.net/AMM.278-280

**The Role of Co-Simulation in the Integrated Design of High-Dynamics Servomechanisms: An Experimental Evaluation**

10.4028/www.scientific.net/AMM.278-280.1758

PRE-PRINT